Geometry and electronic structure of magic iron oxide clusters

Q. Wang, Q. Sun,* M. Sakurai, and J. Z. Yu

Institute for Materials Research, Tohoku University, Sendai 980-77, Japan

B. L. Gu

Institute for Materials Research, Tohoku University, Sendai 980-77, Japan
and Department of Physics, Tsinghua University, Beijing 100084, People's Republic of China

K. Sumiyama and Y. Kawazoe

Institute for Materials Research, Tohoku University, Sendai 980-77, Japan

(Received 1 February 1999)

The magic iron oxide cluster $Fe_{13}O_8$ is found by using a reactive laser vaporized cluster source. From first-principles calculations, the equilibrium geometry is determined to be of D_{4h} symmetry. Comparing with $Fe_{13}O_6$, $Fe_{12}O_9$, and $Fe_{14}O_7$, $Fe_{13}O_8$ has a closed electron configuration in highest occupied molecular orbital (HOMO), a large gap of HOMO-lowest unoccupied molecular orbital, and large binding energy, which suggest that it is most stable, confirming our experimental observation. The main interaction between oxygen and iron atoms in the cluster is the hybridization between O-$2p$ and Fe-$3d$ orbitals. The electronic structure and magnetic properties for this magic iron oxide cluster are discussed in detail. [S0163-1829(99)01620-3]

I. INTRODUCTION

The interaction between substance and oxygen is one of the most important chemical processes to understand corrosion, biological oxygen transport, and oxide film formation. The interest and the richness of this field lie in its interdisciplinary nature and in the diversity of questions it raises, both on fundamental and on applied levels. In recent years, with the new advent of flexible and precise experimental techniques, the studies on oxidation of clusters also have attracted great attention: Fe_n,[1–3] Li_n,[4–6] Cs_n,[7,8] Mn_n,[9,10] Al_n,[11] Si_n,[12,13] and Ba_n clusters.[14,15] Of all the clusters, Fe-O clusters are of particular interest because of their diverse physical and chemical behaviors, and the belief that well-controlled studies on iron oxide clusters not only provide a new avenue to obtain detailed information about the interaction between oxygen and iron but also provide models for iron oxide materials[16] and iron oxide surfaces.[17–19] Small iron oxide clusters have been extensively studied by Wang and his co-workers;[1–3] the photoelectron spectra for $Fe_mO_n^-$ ($m=1-4$, $n=1-6$) indicated that there exist sequential oxygen atom chemisorptions on the surfaces of small iron clusters, which provide novel model systems to understand the electronic structure of bulk iron oxides.[1] However, no studies on larger iron oxide clusters have been reported to our knowledge.

Recently, we have produced iron oxide clusters by using reactive laser vaporized cluster source, where a pulsed second harmonic of Nd:YAG laser was used for vaporization of an iron rod. Metal vapor was cooled by He gas injected from a pulsed gas valve synchronizing with a vaporization laser, and oxygen gas was continuously introduced through a small orifice into a cluster formation cell with 10^3 mm^3 in volume, where the oxygen gas flow rate was changed from 0.0 to 3.0 SCCM controlled by a needle valve and a mass flow meter.

Details of this experiment will be published elsewhere.[20] Figure 1 shows the mass spectra of the Fe_m and Fe_mO_n clusters with different oxygen gas flow rates, from which the following interesting features can be seen: for pure iron clusters, Fe_7, Fe_{13}, Fe_{15}, Fe_{19}, and Fe_{23} are stable; for iron oxide clusters, $Fe_{13}O_8$ is a magic cluster, found in experiment.[20] Why is it magic? What is the geometry, and what are the electronic structure and magnetic properties of this interesting magic iron oxide cluster? In this paper we try to answer these questions by using the first-principles method.
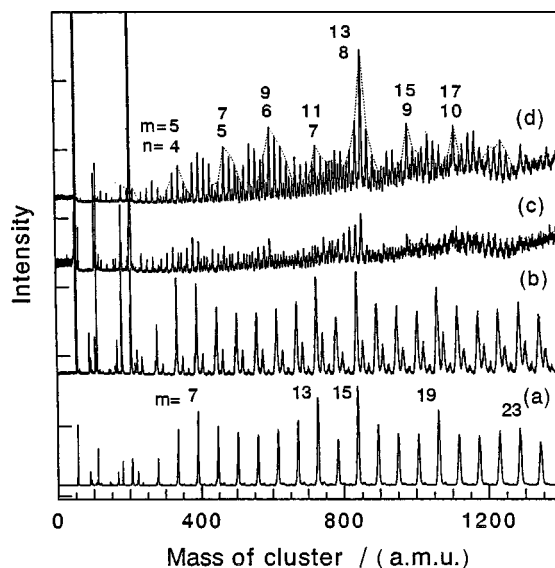

FIG. 1. Time-of-flight mass spectra of positively ionized Fe_m and Fe_mO_n clusters produced by a reactive vaporization cluster source with oxygen flow of (a) 0.0 SCCM, (b) 0.1 SCCM, (c) 0.6 SCCM, and (d) 1.2 SCCM. The dotted line connects the observed peaks corresponding to the clusters having an odd number of iron atoms (m = odd).
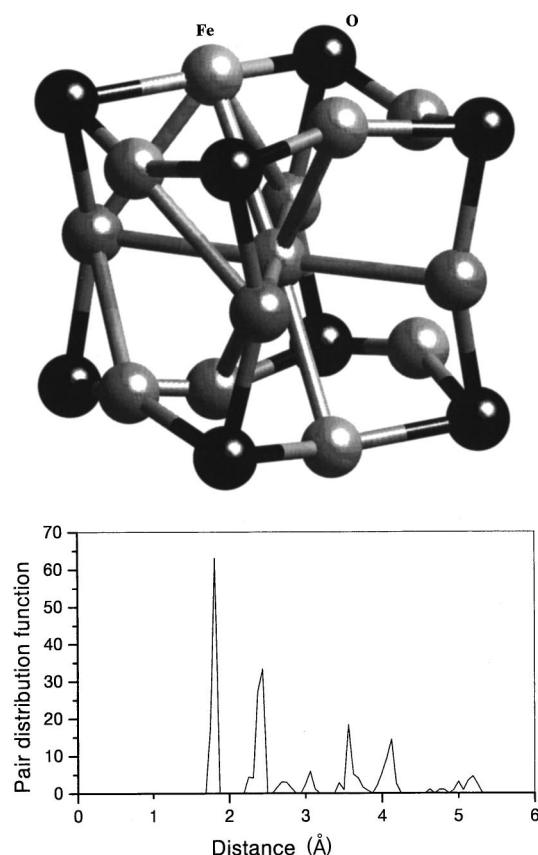
FIG. 2. (a) Optimized structure of $Fe_{13}O_8$ from the initial configuration I. (b) The pair distribution function.

II. THEORETICAL METHOD

Ab initio methods based on density-functional theory (DFT) are well established tools to study the structures and properties of materials. As for structure optimization, the plane-wave basis and pseudopotential method combined with DFT has provided a simple framework, in which the calculation of the Hellmann-Feynman force is greatly simplified so that extensive geometry optimization is possible. To determine the geometry of a $Fe_{13}O_8$ cluster, we used a more
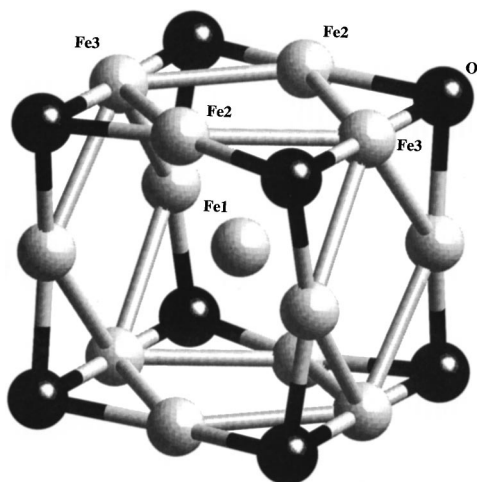

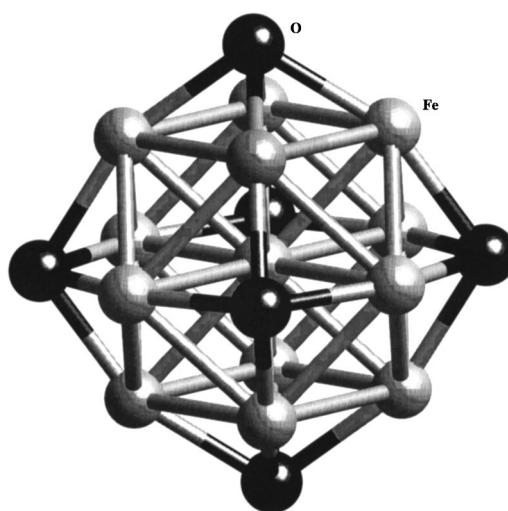FIG. 3. Optimized structure of $Fe_{13}O_8$ from the initial configuration II.

FIG. 4. Optimized structure of $Fe_{13}O_6$.

powerful *ab initio* ultrasoft pseudopotential scheme with plane-wave basis[21,22] [Vienna *Ab initio* Simulation Program (VASP)],[21,22] in which the finite-temperature local-density functional theory developed by Mermin[23] is used, and variational quantity is the electronic free energy. Finite temperature leads to broadening of the one-electron levels that is very helpful to improve the convergence of Brillouin-zone integrations. The electron-ion interaction is described by a fully nonlocal optimized ultrasoft pseudopotential,[24,25] which has been extensively tested for transition metals.[26] The minimization of the free energy over the degrees of freedom of electron densities and atomic positions is performed using the conjugate-gradient iterative minimization technique.[27] In the optimizations, the cluster is placed in a cubic cell with edge length of 14 Å, which is sufficiently large to make dispersion effects negligible, in such a big supercell only the Γ point can be used to represent the Brillouin zone. The cutoff energy used was 400 eV in the plane-wave expansion of the pseudowave functions, which is large enough to obtain a good convergence, and the exchange-correlation energy of valence electrons is adopted in the form of Ceperly and Daler[28] as parametrized by Perdew and Zunger.[29] The structure optimization was symmetry unrestricted, and the optimization was terminated when all the forces acting on the atoms are less than 0.03 eV/Å.
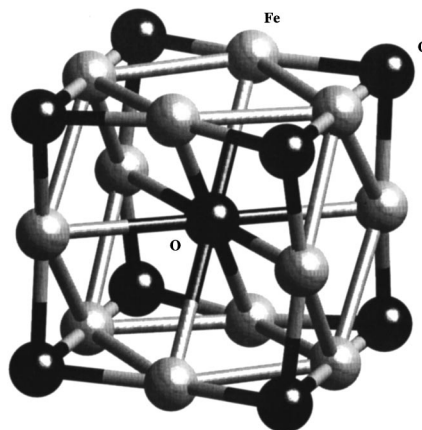

FIG. 5. Optimized structure of $Fe_{12}O_9$.

TABLE I. Electronic structures for Fe_mO_n clusters.

| Cluster | HOMO | | | | | LUMO | | | |
	Spin	Energy	Symbol	Electrons	Configuration	Energy	Symbol	Spin	Δ
$Fe_{13}O_8$	−	−6.5010	a_g	1	Closed	−6.400	a_g	−	0.101
$Fe_{13}O_6$	+	−7.9917	t_g	2	Open	−7.9755	e_g	−	0.016
$Fe_{12}O_9$	−	−6.3979	a_g	1	Closed	−6.3900	a_g	−	0.008

In order to obtain more detailed information on the electronic and magnetic properties, the numerical atomic wave functions are used as the basis set for the expansion of wave functions. The group theory is used to symmetrize the basis functions, which transforms as one of the irreducible representations of the point group of the cluster.[30] The optimized structure with VASP is adopted, and the $3d,4s,4p$ orbitals in Fe, and $2s$ and $2p$ orbitals in O atom are used as the basis set, and the cluster spin orbitals are expanded in a linear combination of the symmetrized basis functions. The Kohn-Sham equation is solved self-consistently with the discrete variational method.[31]

III. RESULTS AND DISCUSSIONS

In order to test our calculations, we first performed calculations on an FeO molecule. The obtained equilibrium bond length is 1.606 Å which is in agreement with the experimental result of 1.618 Å.[32]

It is well known that for an Fe_{13} cluster, there are two
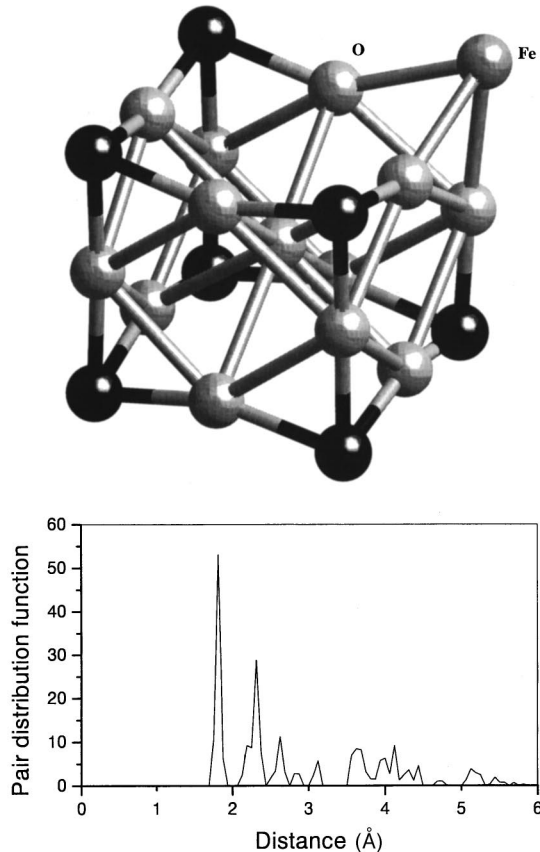

FIG. 6. (a) Optimized structure of $Fe_{14}O_7$. (b) The pair distribution function.

high symmetry structures: icosahedron (I_h) and cuboctahedron (O_h), the former is more stable than the latter, but the difference in total binding energy is small (less than 1.0 eV), which is also confirmed by our calculations. Therefore we start with these two structures to search for the stable structure of $Fe_{13}O_8$. In the icosahedron Fe_{13} cluster, there are 8 nonadjacent triangles among the 20 triangle surfaces. From the previous study on small iron oxide cluster[1] and for the sake of symmetry, we can assume that the 8 oxygen atoms are capped to the 8 nonadjacent triangle surfaces of icosahedron (configuration I). In cuboctahedron Fe_{13} cluster, there are 8 threefold adsorption sites and 6 fourfold adsorption sites, the 8 oxygen atoms are assumed to occupy the 8 threefold adsorption sites (configuration II). We fully optimize these two configurations without any symmetry restrictions. For configuration I, the final structure gives the total binding energy of 117.7 eV, but without any symmetry as shown in Fig. 2(a), the average distance between oxygen and central Fe atom is 3.087 Å, the average distance between Fe and central Fe atom is 2.387 Å, and the average Fe-O bond length is 1.835 Å. Figure 2(b) gives the pair distribution function of this structure. For configuration II, the final structure has D_{4h} symmetry, in which there are three nonequivalent Fe atoms: central Fe atom (labeled as Fe1), surface Fe2 and Fe3, as shown in Fig. 3. The bond lengths and bond angles are as follows: $r_{O-Fe1}=3.141$ Å, $r_{O-Fe2}=1.848$ Å, $r_{O-Fe3}=1.807$ Å, $\angle$O-Fe2-O$=178.4°$, and $\angle$O-Fe3-O $=159.1°$. The total binding energy is 118.6 eV, which is more stable than the former one. Comparing Fig. 2(a) and Fig. 3, it can be found that the appearances of these two structures are similar with each other.

The next question is why is $Fe_{13}O_8$ magic, and not other component clusters, e.g., $Fe_{13}O_6$, $Fe_{12}O_9$, and $Fe_{14}O_7$? Because in a cuboctahedron Fe_{13} cluster, there are 6 fourfold adsorption sites, which could make a possible candidate of $Fe_{13}O_6$. What about $Fe_{13}O_6$? We optimized this cluster, and the final structure is given in Fig. 4, which has O_h symmetry, where the Fe-O bond length is 1.957 Å, Fe-Fe bond length is 2.297 Å, and the total binding energy is 99.513 eV, which is less stable than $D_{4h}Fe_{13}O_8$. In order to further check the

TABLE II. Main orbital components (%) of HOMO and LUMO for Fe_mO_n clusters.

| Cluster | Symmetry | HOMO | | | LUMO | |
		O-$2p$	Fe-$4p$	Fe-$3d$	Fe-$4p$	Fe-$3d$
$Fe_{13}O_8$	D_{4h}			95.4		90.6
$Fe_{13}O_6$	O_h	16.1		83.2		98.7
$Fe_{12}O_9$	D_{4h}		8.3	90.6	8.4	88.6

TABLE III. Occupation numbers and moments of atomic orbitals in $Fe_{13}O_8$ clusters with D_{4h} symmetry, where the numbers in brackets are moments (in μ_b), δq is the net charge, and the orbitals are $3d,4s,4p$ for Fe atom, and $2s,2p$ for O atom.

Atom	$3d$	$4s(2s)$	$4p(2p)$	δq	μ
Fe1	6.6698	0.9379	2.0515	-1.65918	
	(2.4697)	(-0.057)	(0.2034)		(2.6161)
Fe2	6.4173	0.5684	0.4845	0.52984	
	(2.2377)	(0.0083)	(-0.0191)		(2.2269)
Fe3	6.4786	0.6550	0.3809	0.4856	
	(1.5940)	(-0.0042)	(0.005)		(1.5903)
O		1.9002	4.6650	-0.5652	
		(-0.0043)	(-0.0947)		(-0.099)

stability of the cluster, in $Fe_{13}O_8$, we use one oxygen atom to replace the central Fe atom forming $Fe_{12}O_9$, or use one Fe atom to replace one oxygen atom forming $Fe_{14}O_7$. The optimized structure for $Fe_{12}O_9$ is shown in Fig. 5, which has D_{4h} symmetry, similar to $Fe_{13}O_8$, the distance to the central O atom for Fe2 and Fe3 is 2.372 and 2.546 Å, respectively, and the total binding energy is 114.5 eV. The optimized structure for $Fe_{14}O_7$ is shown in Fig. 6(a), which has no symmetry. The Fe-O bond length changes from 1.769 to 1.88 Å, and the Fe-Fe bond length varies in the region of 2.176 to 2.414 Å. The total binding energy is 114.4 eV, and Fig. 6(b) gives the
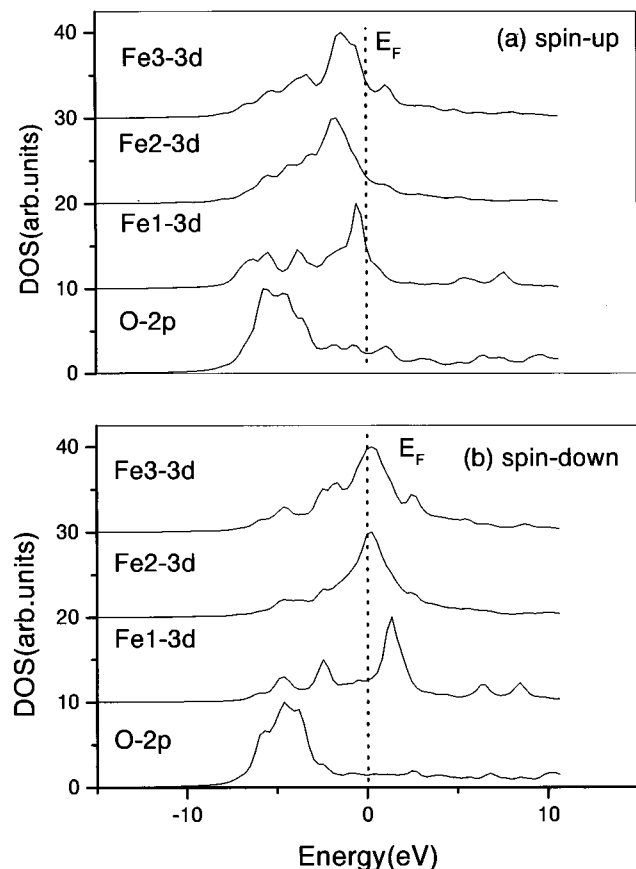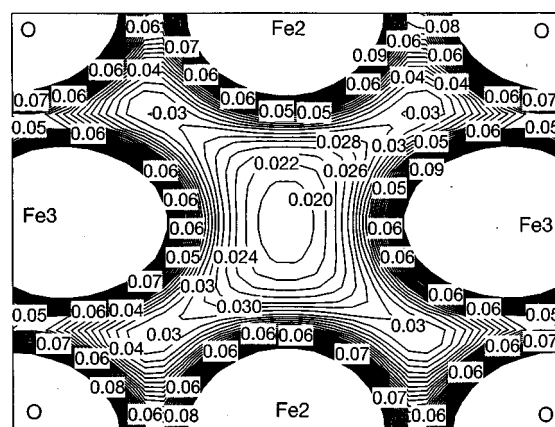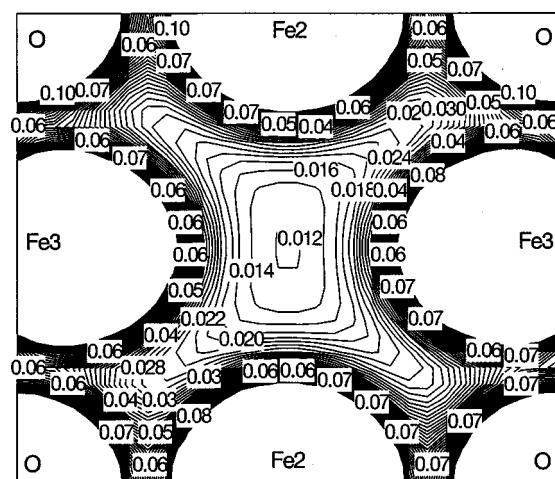

(a)

(b)

FIG. 8. Charge density distribution of spin-up (a) and spin-down (b) on the Fe2-Fe3-O plane in $Fe_{13}O_8$ with D_{4h}.

FIG. 7. Partial density of states for O-$2p$, Fe1-3d, Fe2-3d, and Fe3-3d in $Fe_{13}O_8$ with D_{4h} symmetry, (a) spin-up and (b) spin-down.

pair distribution function of this cluster. Comparing the binding energies of $Fe_{13}O_8$, $Fe_{13}O_6$, $Fe_{12}O_9$, and $Fe_{14}O_7$, we can see that $Fe_{13}O_8$ is most stable. Therefore it is determined to be magic, confirming our experimental result.

Table I lists some numerical results on the electronic structures of clusters with symmetry, and the corresponding orbital percentage components for the highest occupied molecular orbital (HOMO) and the lowest unoccupied molecular orbital (LUMO) are given in Table II. We can see that the $Fe_{13}O_8$ cluster has a closed electron configuration in HOMO and a large gap between HOMO and LUMO, which makes this cluster stable. It can also be found that different components in a cluster result in a different electronic structure. For example, in an $Fe_{13}O_8$ cluster with D_{4h} symmetry, the HOMO is contributed by 95.4% Fe-$3d$ orbitals, and LUMO by 90.6% Fe-$3d$ orbitals; in an $Fe_{13}O_6$ cluster with O_h symmetry, the HOMO is a mixture of 16.1% O-$2p$ orbitals and 83.2% Fe-$3d$ orbitals, and LUMO consists of 98.7% Fe-$3d$ orbitals; in an $Fe_{12}O_9$ cluster with D_{4h} symmetry, the HOMO is composed of 8.3% Fe-$4p$ orbitals and 90.6% Fe-$3d$ orbitals, and LUMO consists of 88.6% Fe-$3d$ orbitals and 8.4% Fe-$4p$ orbitals; the common feature is that LUMO is

nearly d type, quite different from what has been found in bulk Fe_2O_3, where the lowest unoccupied state is not Fe $3d$-like but is the bottom of the Fe $4s$ band.[33]

Table III shows the occupation numbers and moments of atomic orbitals of the $Fe_{13}O_8$ cluster with D_{4h} symmetry, from which we can obtain the following results.

(1) Comparing with the electronic configurations of $3d^6 4s^2 4p^0$ and $2s^2 2p^4$ for the isolated Fe and O atoms, we find that the O atom is an electron acceptor with 0.56517 electrons transferred from Fe2 and Fe3 atoms. Moreover, the $3d$ and $4p$ orbital of the central Fe1 atom also gets electrons from Fe2 and Fe3. This is due to the following facts: the p and d orbitals of the central atom in D_{4h} structure will be split as follows: the three p orbitals (p_x, p_y, p_z) are split into e_u orbital (p_x, p_y) and a_{2u} (p_z); the five d orbitals $(d_{xy}, d_{yz}, d_{xz}, d_{z^2}, d_{x^2-y^2})$ are split into e_g orbitals (d_{yz}, d_{xz}), b_{2g} orbital (d_{xy}), b_{1g} orbital $(d_{x^2-y^2})$, and a_{1g} orbitals (d_{z^2}), such splittings are favorable for decreasing the energy, and electrons transferring to these orbitals make the system more stable.

(2) Oxygen atoms are weakly polarized antiferromagnetically.

(3) Fe1, Fe2, and Fe3 atoms have magnetic moments of 2.6161, 2.2269, and $1.5902\mu_B$, respectively. The magnetic moment changing in this order is attributed to the fact that its distance to the oxygen atom gradually decreases as $r_{O-Fe1} > r_{O-Fe2} > r_{O-Fe3}$. From the local densities of state for Fe1, Fe2, Fe3, and O atoms, as shown in Fig. 7, we can see that the main interaction between Fe and O atoms is the hybridization between $3d$ orbitals of the Fe atom and $2p$-O orbitals. Shorter bond length makes stronger hybridization, accordingly, the magnetic moment decreases, and the average moment of the Fe atom in this cluster is $2.061\mu_B$.

Figures 8(a) and 8(b) give the charge density distribution of spin-up and spin-down on the Fe2-Fe3-O plane in $Fe_{13}O_8$ with D_{4h} symmetry.

It is well known that the magic number for clusters depends on the chemistry of elements. For rare-gas atoms, close packing of atoms gives rise to magic numbers of 13, 55, 143,...;[34] for simple alkali metals, magic numbers at 2, 8, 20,... are brought about by electronic shell closure;[35] for ionically bonded clusters such as alkali halide $(NaCl)_x$ Ref. 36 and $(MgO)_5$,[37] the magic numbers are 4, 23, 22, 37,..., which can be understood as originating from the fcc structure of the bulk systems and by realizing that ultrastable clusters are fragments of their bulk; but for transition metal-oxide clusters, the situation is more complicated, different magic number can be exhibited,[38–40] and more richness in physics and chemistry would exist.

In this paper, by the first-principles calculations, the equilibrium geometry, and electronic structures of $Fe_{13}O_8$, which was found as a magic cluster by our experiment, are studied and the stability of this cluster is confirmed.

*Author to whom correspondence should be addressed.

[1] L. S. Wang, H. B. Wu, and S. R. Desai, Phys. Rev. Lett. **76**, 4853 (1996).

[2] L. S. Wang, J. W. Fan, and L. Lou, Surf. Rev. Lett. **3**, 695 (1996).

[3] H. B. Wu, S. R. Desai, and L. S. Wang, J. Am. Chem. Soc. **118**, 5296 (1996).

[4] Fabio Finocchi and Claudine Noguera, Phys. Rev. B **57**, 14 646 (1998).

[5] C. Brechignac, Ph. Cahuzac, M. de Frutos, and P. Garnier, Z. Phys. D **42**, 303 (1997).

[6] V. Bonacic-Koutecky, J. Pittner, R. Pou-Amerigo, and M. Hartmann, Z. Phys. D **40**, 445 (1997).

[7] T. Bergmann and T. P. Martin, J. Chem. Phys. **90**, 2848 (1989).

[8] H. G. Limberger and T. P. Martin, J. Chem. Phys. **90**, 2979 (1989).

[9] P. J. Ziemann and A. W. Castlemann, Jr., J. Chem. Phys. **94**, 718 (1991).

[10] S. K. Nayak and P. Jena, Phys. Rev. Lett. **81**, 2970 (1998).

[11] S. R. Desai, H. B. Wu, and L. S. Wang, J. Chem. Phys. **106**, 1309 (1997).

[12] L. S. Wang, J. B. Nicholas, M. Dupuis, H. B. Wu, and S. D. Colson, Phys. Rev. Lett. **78**, 4450 (1997).

[13] L. S. Wang, H. B. Wu, S. R. Desai, J. W. Fan, and S. D. Colson, J. Phys. Chem. **100**, 8697 (1996).

[14] V. Boutou, M. A. Lebeault, A. R. Allouche, C. Bordas, F. Pauling, J. Viallon, and J. Chevaleyre, Phys. Rev. Lett. **80**, 2817 (1998).

[15] T. P. Martin and T. Bergmann, J. Chem. Phys. **90**, 6664 (1989).

[16] J. S. Corneille, J. W. He, and D. W. Goodman, Surf. Sci. **338**, 211 (1995).

[17] V. E. Henrich and P. A. Cox, *The Surface Science of Metal Oxides* (Cambridge University Press, Cambridge, England, 1994).

[18] N. G. Conden, Phys. Rev. Lett. **75**, 1961 (1995).

[19] R. Wiesendanger, Science **255**, 583 (1992).

[20] M. Sakurai, Q. Sun, K. Sumiyama, and Y. Kawazoe (unpublished).

[21] G. Kresse and J. Hafner, Phys. Rev. B **47**, 558 (1993); **49**, 14 251 (1994).

[22] G. Kresse and J. Furthmüller, Phys. Rev. B **54**, 11 169 (1996).

[23] N. D. Mermin, Phys. Rev. A **137**, 1141 (1965).

[24] D. Vanderbilt, Phys. Rev. B **41**, 7892 (1990).

[25] G. Kresse and J. Hafner, J. Phys.: Condens. Matter **6**, 8245 (1994).

[26] E. G. Moroni, G. Kresse, and J. Furthmüller, Phys. Rev. B **56**, 15 629 (1997).

[27] M. C. Payne, M. P. Teter, D. C. Allan, T. A. Arias, and J. D. Joannopoulos, Rev. Mod. Phys. **64**, 1045 (1992).

[28] D. M. Ceperley and B. J. Daler, Phys. Rev. Lett. **45**, 566 (1980).

[29] J. P. Perdew and A. Zunger, Phys. Rev. B **23**, 5048 (1981).

[30] Q. Sun, X. G. Gong, Q. Q. Zheng, D. Y. Sun, and G. H. Wang, Phys. Rev. B **54**, 10 896 (1996).

[31] D. E. Ellis and G. S. Painter, Phys. Rev. B **2**, 2887 (1970).

[32] A. S-C. Cheung, R. M. Gordon, and A. J. Merer, J. Mol. Spectrosc. **87**, 289 (1991).

[33] A. Fujimori, M. Saeki, N. Kimizuka, M. Taniguchi, and S. Suga, Phys. Rev. B **34**, 7318 (1986).

[34] I. A. Harris, R. S. Kidwell, and J. A. Northby, Phys. Rev. Lett. **53**, 2390 (1984).

[35] W. D. Knight, Phys. Rev. Lett. **52**, 2141 (1984).

[36] Y. J. Twu, Phys. Rev. B **42**, 5306 (1990).

[37] Y. J. Ziemann and A. W. Castlemann, Jr., J. Chem. Phys. **94**, 718 (1991).

[38] P. J. Ziemann and A. W. Castlemann, Jr., Phys. Rev. B **46**, 13 480 (1992).

[39] S. Veliah, R. Pandey, Y. S. Li, J. Newsam, and B. Vessal, Chem. Phys. Lett. **235**, 53 (1995).

[40] S. Veliah, K. H. Xiang, R. Pandey, J. M. Recio, and J. Newsam, J. Phys. Chem. B **102**, 1126 (1998).